Talanta 125 (2014) 159–166

Contents lists available at ScienceDirect

Talanta

journal homepage: www.elsevier.com/locate/talanta

Array of peptide-modified electrodes for the simultaneous determination of Pb(II), Cd(II) and Zn(II)

Núria Serrano [a,b], Beatriz Prieto-Simón [b,c], Xavier Cetó [b], Manel del Valle [b,*]

[a] Department of Analytical Chemistry, Faculty of Chemistry, Universitat de Barcelona, Martí i Franquès 1-11, 08028 Barcelona, Spain
[b] Sensors and Biosensors Group, Department of Chemistry, Universitat Autònoma de Barcelona, Edifici Cn, 08193 Bellaterra, Spain
[c] Mawson Institute, University of South Australia, Mawson Lakes, South Australia 5001, Australia

ARTICLE INFO

Article history:
Received 2 December 2013
Received in revised form
13 February 2014
Accepted 20 February 2014
Available online 28 February 2014

Keywords:
Peptide-modified sensors
Electrochemical grafting
Metal determination
Stripping voltammetry
Quatrilinear data
Artificial neural network

ABSTRACT

This paper reports the development of three peptide modified sensors in which glutathione (GSH) and its fragments Cys–Gly and γ-Glu–Cys were immobilized respectively through aryl diazonium electrochemical grafting onto the surface of graphite–epoxy composite electrodes (GEC), and used for the simultaneous determination of Cd(II), Pb(II) and Zn(II). The concentration interval ranged from 0.1 to 1.5 μmol L^{-1} for each metal, and the technique used was differential pulse adsorptive stripping voltammetry. This study aimed to the comparison of the information provided by one single modified electrode at both fixed and multiple pH values (pH 6.8, 7.5 and 8.2) for the simultaneous determination of the three metals, with those supplied by the three-sensor array at multiple pH values. For the processing of the voltammograms, the fast Fourier transform was selected as the preprocessing tool for data compression coupled with an artificial neural network for the modeling of the obtained responses.

1. Introduction

Monitoring levels of metal ions in aquatic ecosystems and soils is of great importance in recent years from environmental and biological point of view. In this sense, the use of chemically modified electrodes, and particularly peptide modified electrodes for the detection and quantification of metal ions in natural samples is an area of major concern [1–3]. Peptides are effective ligands for a great variety of metal ions. Their ability to bind these metal ions is a consequence of the great number of potential donor atoms they contain, both through the peptide backbone and amino acid side chains [1,2]. The complexation of heavy metals by thiol rich peptides such as glutathione (γ-Glu–Cys–Gly, denoted usually as GSH), its fragments Cys–Gly and γ-Glu–Cys, or oligomers named phytochelatins ($(\gamma\text{-Glu–Cys})_n$–Gly, denoted usually as PC_n), and related molecules has been extensively studied using electroanalytical techniques on mercury [4–13] and bismuth electrodes [14,15] in combination with multivariate data analysis. These works demonstrate that complex formation with the thiol groups from the cysteines plays a crucial role in natural metal binding, and it is important not only for heavy metal detoxification but also for phytoremediation purposes [16–18].

An essential aspect in the design of these electrodes is the molecule immobilization procedure [19]. In this sense, various approaches were described in the literature including the use of gold electrodes and the formation of self-assembled monolayers (SAMs), in which the peptide is immobilized on the electrode surface through the use of anchoring thiol groups. Nevertheless, the peptide immobilization on aryl diazonium salt monolayers anchored on the electrode surface has demonstrated to be an alternative strategy that can overcome the major limitations of thiol SAMs such as the narrow potential range for metal ion detection [20,21].

Peptide modified electrodes can be used for metal determination as a single-electrode sensor or in combination with others forming a multi-sensor array, in which each electrode in the array is modified with different compounds in search for a multivariate response. A multi-electrode array presents some disadvantages over a single sensor in that a multichannel potentiostat to control the potential is required and that the manufacturing time is longer. However, these disadvantages are counterbalanced if the information provided by the electrode array is significantly higher than that obtained from a single electrode. These two approaches were investigated by Ebrahimi et al. for the determination of Cu(II), Cd(II) and Pb(II) using a four gold electrode sensor array modified with D,L-6,8-thioctic acid (TA), TA–Gly–Gly–His, TA–GSH and TA–angiotensin I, or a single electrode modified with the four compounds [22]; the determination required the use of the multivariate chemometric tool partial least squares regression (PLS).

* Corresponding author. Tel.: +34 93 5811017; fax: +34 93 5812477.
E-mail address: manel.delvalle@uab.cat (M. del Valle).

http://dx.doi.org/10.1016/j.talanta.2014.02.052
0039-9140

In this paper, we report the design of three peptide-modified sensors in which GSH, Cys–Gly and γ-Glu–Cys were immobilized on aryl diazonium salt monolayers electrochemically grafted to the surface of graphite–epoxy composite electrodes (GEC) for the simultaneous determination of ppb levels of Cd(II), Pb(II) and Zn (II). The selection of these three peptides is motivated by the fact that previous complexation studies demonstrated that Cys–Gly and γ-Glu–Cys fragments, as well as the pH of the medium play a particular and important role in each metal binding, since the presence of different binding sites in GSH greatly increases the number of possible structures of the complexes [23,24]. In this respect, the aim of the present study is to compare the information about the simultaneous determination of Cd(II), Pb(II) and Zn(II) provided by one peptide-modified sensor at both single and multi-pH values (pH 6.8, 7.5 and 8.2) with that supplied by the three-sensor array at multi-pH values, being the first attempt using quatrilinear data (sample × sensor × potential × pH). An artificial neural network (ANN) model was proposed as a tool to maximize the information obtained from the voltammetric data sets using GSH–GEC, γ-Glu–Cys–GEC and Cys–Gly–GEC sensors that a priori are difficult to interpret.

2. Experimental

2.1. Chemicals

Potassium ferricyanide $K_3[Fe(CN)_6]$, potassium ferrocyanide $K_4[Fe(CN)_6]$, 2-(N-morpholino)-ethanesulfonic acid (MES), potassium dihydrogen phosphate, sodium monophosphate, methanol, perchloric acid, hydrochloric acid, *N*-hydroxysulfosuccinimide (sulfo-NHS), *N*-(3-dimethylaminopropyl)-*N′*-ethylcarbodiimide hydrochloride (EDC) and sodium nitrite were purchased from Sigma (St. Louis, MO, USA). 4-aminobenzoic acid (ABA) was provided by Acros (Geel, Belgium). All other reagents used were from Merck (Darmstadt, Germany) and Fluka (Buchs, Switzerland). All reagents were of analytical grade. Glutathione (GSH), in the reduced form, was provided by Merck with purity greater than 99%. γ-Glu–Cys and Cys–Gly were provided by Sigma with a purity of 80% (as fluoroacetate salt) and 85%, respectively. Pb(II), Cd(II) and Zn(II) stock solutions 10^{-2} mol L^{-1} were prepared from $Pb(NO_3)_2 \cdot 4H_2O$, $Cd(NO_3)_2 \cdot 4H_2O$ and $Zn(NO_3)_2 \cdot 4H_2O$ respectively and standardized complexometrically [25].

Ultrapure water from MilliQ System (Millipore, Billerica, MA, USA) was used in all experiments.

2.2. Apparatus

Differential pulse adsorptive stripping voltammetric (AdSV) measurements were performed in an Autolab System PGSTAT 30 (EcoChemie, The Netherlands), in a multichannel configuration, using GPES Multichannel 4.7 software package (EcoChemie). The voltammetric cell was formed by the three working graphite epoxy electrodes (GECs) modified with GSH, γ-Glu–Cys and Cys–Gly respectively, a commercial platinum counter electrode (Model 52-67, Crison Instruments, Barcelona, Spain) and a double junction Ag/AgCl reference electrode (Thermo Orion 900200, Beverly, MA, USA).

Impedance measurements were performed with an IM6e Impedance Measurement Unit (BAS-Zahner, Kronach Germany) using Thales (BAS-Zahner) software for data acquisition and control of the experiments. A three electrode configuration was used to perform the impedance measurements: a commercial platinum counter electrode, a reference double junction Ag/AgCl electrode and the GEC as the working electrode.

A pH meter GLP 22 (Crison Instruments, Barcelona, Spain) was used for pH measurements.

All measurements were carried out at room temperature (20 °C).

2.3. Procedures

2.3.1. Preparation of graphite epoxy electrodes

Graphite epoxy composite electrodes (GECs) were fabricated using a PVC tube body (6 mm i. d.) and a small copper disk soldered at the end of an electrical connector. The working surface is an epoxy–graphite conductive composite, formed by a mixture of 20% graphite powder (Merck, Darmstadt, Germany) and 80% of epoxy resin, Epotek H77, and its corresponding hardener (both from Epoxy Technology, Billerica, MA, USA), deposited on the cavity of the plastic body [26]. The composite material was cured at 80 °C for 3 days. Prior to their functionalization, the electrode surface was moistened with MilliQ water and then polished on abrasive sandpaper (400, 600, 800, 1000 and 1200 grit) and finally on alumina polishing strips (301044-001, Orion) in order to obtain a reproducible electrochemical surface.

2.3.2. Preparation of modified GECs

The principle of the modification of the GEC is illustrated in Fig. 1, with specific steps described below [27].

2.3.2.1. Diazonium salt electrografting. The in situ generation of the aryl diazonium was performed by adding 5×10^{-3} equivalents of sodium nitrite to an acidic solution (1 M aqueous HCl) of ABA. These solutions were mixed for about 30 min in an ice bath, prior to the electrografting process, conducted by scanning the potential at 0.2 V s^{-1} from 0 V to −1 V for 100 cycles. The functionalized electrodes were thoroughly rinsed with Milli-Q water and methanol to remove the physisorbed compounds.

2.3.2.2. Covalent immobilization of peptides via carbodiimide coupling. The carboxyl groups of the electrografted diazonium salt were activated by incubating the functionalized electrodes in a 26 mM EDC and 35 mM sulfo-NHS solution in 100 mM MES

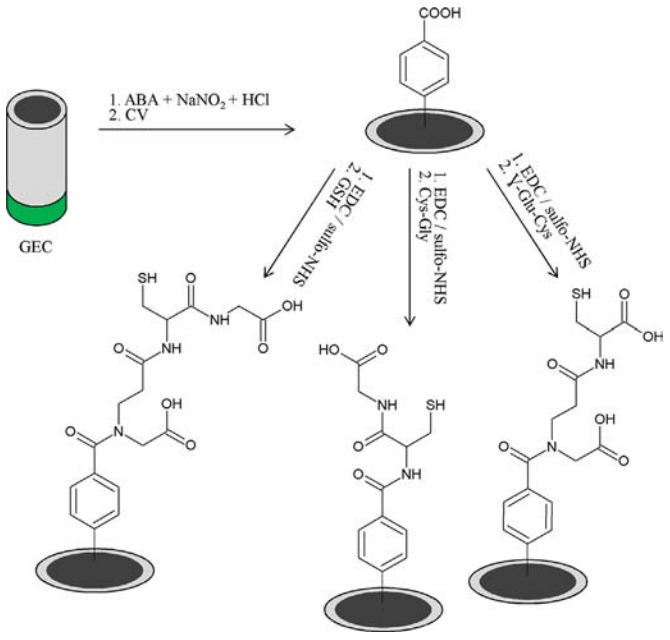

Fig. 1. Scheme of the preparation of GSH–GEC, γ-Glu–Cys–GEC and Cys–Gly–GEC by electrochemical grafting.

buffer (pH 4.5) for 1 h. The activated groups reacted overnight with the amine terminal groups of each peptide (GSH, γ-Glu–Cys, Cys–Gly at 2.9 mg/100 μL in 0.1 M MES buffer) at 4 °C to form amide bonds.

2.3.3. Electrochemical characterization

Electrodes were characterized at each functionalization step using cyclic voltammetry (CV) and electrochemical impedance spectroscopy (EIS). Electrochemical measurements were performed in an unstirred solution of 2 mM ferrocyanide and 2 mM ferricyanide in 100 mM phosphate buffer, pH 7.4. Cyclic voltammograms were obtained by scanning the potential at 0.1 V s^{-1} from −0.2 V to 0.6 V. EIS measurements were performed under open circuit potential conditions. Frequencies from 500 kHz to 0.1 Hz in logarithmic spacing were applied. The AC amplitude was 5 mV.

2.3.4. Voltammetric measurements

Voltammograms were obtained under the following conditions: a deposition potential (E_d) of −1.4 V applied with stirring during a deposition time (t_d) of 300 s followed for a rest period (t_r) of 10 s; a stripping potential swept from −1.4 V to −0.5 V vs. Ag/AgCl, using a step potential of 4 mV and pulse amplitude of 50 mV.

All experiments were carried out without any oxygen removal.

Prior to sample measurements, the electrodes were scanned in buffer solution in order to get stable voltammetric responses.

In order to eliminate the remaining bound metals from the electrode an electrochemical cleaning stage was considered between measurements. This stage is performed applying a conditioning potential (E_{cond}) of 0.5 V for 15 s after each measurement, in a cell containing 0.1 mol L^{-1} $HClO_4$ [28].

2.3.5. Preparation of metals mixtures samples

From the prepared metal stock solutions, a total set of 36 samples were manually prepared by appropriate dilution for each of the considered pH values (6.8, 7.5 and 8.2). The set of samples was divided into two data subsets: a training subset formed by 27 samples (75%), which were distributed in a cubic design [29] and used to establish the response model; plus 9 additional samples (25%) for the testing subset, randomly distributed along the experimental domain, and used to evaluate the model predictive response. Table 1 shows the specific concentrations of the three considered metals in the 36 samples prepared, at 3 pHs 6.8, 7.5 and 8.2. Maleic acid–KOH buffer solution 0.1 mol L^{-1} (pH 6.8) and Tris (hydroxymethyl) aminomethane–HCl buffer solution 0.1 mol L^{-1} (pH 7.5 and pH 8.2) were used for pH control.

Table 1
Concentration information for the complete data set, all values are in ppb. One stripping voltammogram was measured on GSH–GEC, Cys–Gly–GEC and γ-Glu–Cys–GEC sensors for each combination of the three metal concentrations at pH 6.8, 7.5 and 8.2.

Pb(II)	Cd(II)	Zn(II)
Training subset sample concentrations (ppb)		
20.7	23.3	34.7
31.9	41.5	66.4
43.0	59.7	98.1
54.2	77.8	31.2
65.3	96.0	62.9
76.5	114.1	94.6
87.7	132.3	27.7
98.8	150.5	59.4
110.0	168.6	91.1
121.1	17.3	24.2
132.3	35.5	55.9
143.4	53.6	87.5
154.6	71.8	20.6
165.8	89.9	52.3
176.9	108.1	84.0
188.1	126.2	17.1
199.2	144.4	48.8
210.4	162.6	80.5
221.5	11.2	13.6
232.7	29.4	45.3
243.9	47.6	77.0
255.0	65.7	10.1
266.2	83.9	41.8
277.3	102.0	73.5
288.5	120.2	6.5
299.6	138.4	38.2
310.8	156.5	69.9
External test subset of samples (ppb)		
179.9	54.5	40.0
148.1	125.2	75.7
202.0	72.7	28.5
80.7	43.4	42.3
189.0	100.2	65.6
125.3	161.7	85.6
88.3	66.2	53.8
63.9	85.5	92.8
113.7	133.4	82.0

2.4. Data processing

A known problem when voltammetric sensors are used is the large data record generated which hinders their treatment; especially if ANNs are to be used, in which case departure information needs to be preprocessed [30]. Besides avoiding saturating the associated model, this step may also help to gain advantages in training time, to avoid redundancy in input data and to obtain a model with better generalization ability.

Hence, for the construction of the chemometric model, voltammetric data was first compressed employing fast Fourier transform (FFT) [30]. By compromising between the reconstruction degree and the number of obtained coefficients, raw voltammetric data was compressed up to only 8 coefficients without any loss of significant information, which allowed for a compression of the original information up to 96.1%. Afterwards, the obtained coefficients were used as inputs in the ANN model which, after its optimization, allowed the quantification of the different metals.

The chemometric processing of the data described above was performed by specific routines written by the authors using MATLAB 7.1 (MathWorks, Natick, MA) and its Neural Network toolbox. Additionally, Sigmaplot (Systat Software Inc, CA) was also used for graphic representations of data and results.

3. Results and discussion

3.1. Electrochemical characterization: CV and EIS analysis

CV and EIS data were used to characterize each step of functionalization. After electrografting, the electrochemical response for the redox probe ferrocyanide/ferricyanide and the potential peak separation between the anodic and cathodic peaks was investigated using CV. Electrografting resulted in decreasing current as expected (Fig. 2a). Covalent binding of peptides also resulted in lower current peaks, as shown in Fig. 2a for GSH. GSH, γ-Glu–Cys and Cys–Gly have an isoelectric point lower than the working pH (7.4), and thus, they remained negatively charged under working conditions, leading to the decrease of the current measured for the oxidation/reduction of the redox probe because of electrostatic repulsion. EIS was also used to confirm the electrografting and peptide binding. The recorded

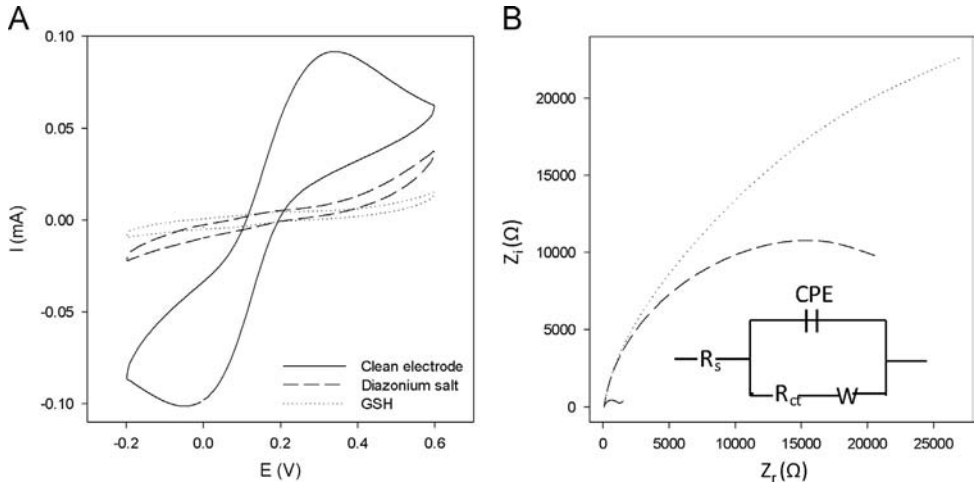

Fig. 2. (A) CVs and (B) Nyquist impedance plots recorded at electrodes modified with electrografted diazonium salts and covalently bound GSH. Measurements were performed in a 2 mM ferrocyanide/ferricyanide solution in phosphate buffer. Inset in (B): equivalent circuit used to fit experimental data.

impedance spectra were fitted to a Randles circuit, corresponding to a basic equivalent circuit that includes the solution resistance (R_s), the charge transfer resistance (R_{ct}), the Warburg impedance (W) and a constant phase element (CPE, originated by non-idealities in the electrode surface) (Fig. 2b). The R_{ct} values obtained from the diameter of the semicircle of the Nyquist plots in Fig. 2b showed a significant increase after electrografting, from 1090 Ω for a bare electrode to 20,093 Ω for a diazonium salt-modified electrode. Binding of the peptide led to a further increase in R_{ct} that confirmed the immobilization of the peptide on the electrode surface.

3.2. Voltammetric responses

The selected E_d, t_d and t_r were firstly optimized to ensure the detection of each metal at each modified electrode in the selected concentration range (data not shown), being for all cases a E_d of −1.4 V applied with stirring during a t_d of 300 s and followed for a t_r of 10 s.

Applying the described procedure, the set of 36 samples detailed in Table 1 was measured at pH values of 6.8, 7.5 and 8.2 using the three modified electrodes: GSH–GEC, γ-Glu–Cys–GEC and Cys–Gly–GEC, obtaining a whole stripping voltammogram for each of the sensors. Fig. 3 displays, as an example, the obtained voltammograms for the complete data set using the GSH–GEC sensor for the simultaneous determination of Pb(II), Cd(II) and Zn(II) at the different pH values. At pH 6.8 (Fig. 3a) Cd(II) and Pb(II) ions exhibit at ca. −0.89 V and −0.65 V respectively an unique, well defined and undistorted peak in the wide range of metal concentration, but in agreement with previous works [24] no signal due to Zn(II)-ion was detected. Moreover in the concentration range from 0.1 to 1.5 μmol L^{-1} for Cd(II) and Pb(II) a linear response with the peak area of each metal was obtained. However, the increase of the metal concentration produces a gradual peak potential shift in both metal signals to more positive potentials. At pH 7.5 (Fig. 3b) the voltammograms displayed no differences in Pb(II) peak shape and peak potential shift with the signals measured at pH 6.8, whereas Cd(II) presents a more distorted signal with an unique or two overlapping peaks depending on the metal concentration range. In agreement with the aforementioned study [24], a wide signal related to Zn(II)-ions appears at ca. −1.16 V when the pH value increases. The total area of the voltammograms of each metal is again linear with the metal concentration from 0.1 to 1.5 μmol L^{-1} for Pb(II), Cd(II) and Zn(II).

Finally, voltammograms obtained at pH 8.2 (Fig. 3c) show that pH value does not affect the peak shape and position of Pb(II)-ion, while Cd(II) and Zn(II) signals are increasingly distorted and overlapping. Even so, the same linear dependence between total peak areas and concentrations was observed inside the same ranges for Pb(II), Cd(II) and Zn(II).

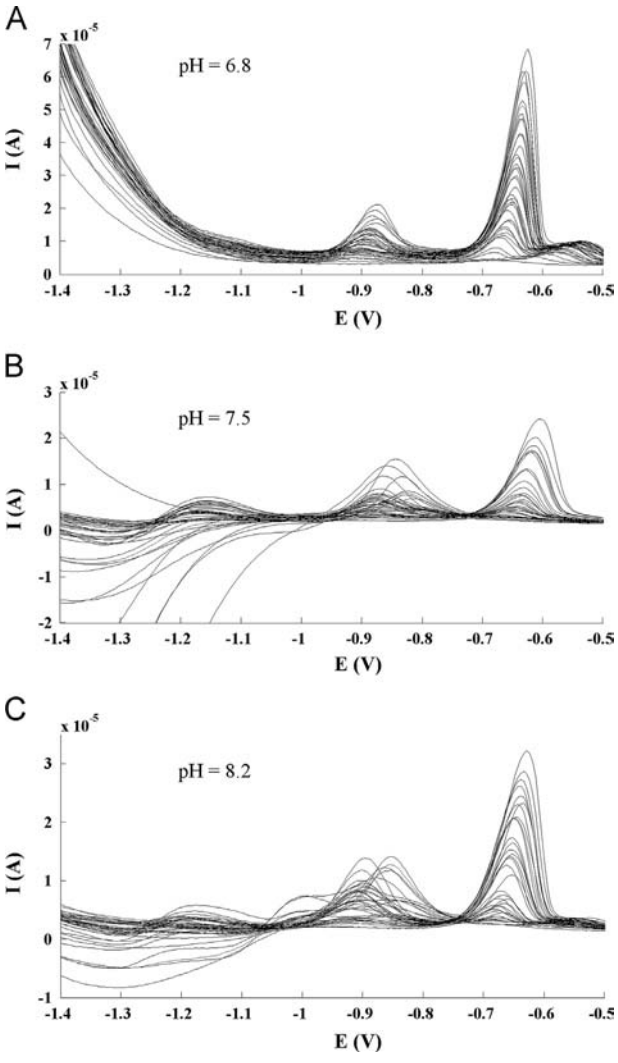

Fig. 3. Differential pulse adsorptive stripping voltammograms of Pb(II), Cd(II) and Zn(II) recorded on a GSH–GEC sensor at the three selected pH's ((A) 6.8, (B) 7.5, and (C) 8.2) using a E_d of −1.40 V during 300 s and t_r of 10 s.

Table 2
Peak potentials and sensitivities obtained from the complete voltammetric data set measured on GSH–GEC, Cys–Gly–GEC and γ-Glu–Cys–GEC sensors at pH 6.8, 7.5 and 8.2.

	Pb (II)			Cd (II)			Zn (II)		
	GSH	Cys-Gly	γ-Glu-Cys	GSH	Cys-Gly	γ-Glu-Cys	GSH	Cys-Gly	γ-Glu-Cys
pH 6.8									
Potential (V)[a]	-0.65 ± 0.01	-0.65 ± 0.01	-0.66 ± 0.01	-0.89 ± 0.01	-0.89 ± 0.01	-0.90 ± 0.01	n.d.	n.d.	n.d.
Sensitivity (nA ppb^{-1})[b]	12.0 ± 0.6	9.9 ± 0.5	7.8 ± 0.8	6.8 ± 0.4	6.4 ± 0.5	6.3 ± 0.7			
pH 7.5									
Potential (V)[a]	-0.64 ± 0.02	-0.63 ± 0.01	-0.64 ± 0.02	-0.88 ± 0.01	-0.88 ± 0.01	-0.88 ± 0.01	-1.16 ± 0.01	-1.15 ± 0.01	-1.16 ± 0.01
Sensitivity (nA ppb^{-1})[b]	5.8 ± 0.7	6 ± 1	6 ± 1	6.8 ± 0.4	6.4 ± 0.8	5.9 ± 0.7	11 ± 1	12 ± 2	8 ± 2
pH 8.2									
Potential (V)[a]	-0.66 ± 0.02	-0.65 ± 0.01	-0.65 ± 0.01	-0.89 ± 0.02	-0.89 ± 0.03	-0.89 ± 0.03	-1.19 ± 0.01	-1.18 ± 0.02	-1.19 ± 0.01
Sensitivity (nA ppb^{-1})[b]	6 ± 1	6.0 ± 0.6	5.9 ± 0.7	6 ± 1	5.4 ± 0.5	5.0 ± 0.6	8 ± 1	9 ± 1	6 ± 1

n.d.: not detected

[a] Value is the mean of 36 standard concentrations of Pb(II), Cd(II) and Zn(II), and the standard deviations obtained.
[b] Value obtained from the slope of the calibration curve and its corresponding standard deviation.

Similar voltammetric responses for Pb(II), Cd(II) and Zn(II) were also observed using γ-Glu–Cys–GEC and Cys–Gly–GEC sensors at the three measured pH values.

Table 2 summarizes the mean of the peak potential and the sensitivities computed from the slope of the calibration curve of each metal at the three measured pH values using the three modified electrodes: GSH–GEC, γ-Glu–Cys–GEC and Cys–Gly–GEC. As it can be seen, at pH 6.8 Pb(II) regardless of the used sensor has better sensitivity than Cd(II). When the pH value is 7.5 the sensitivity for Zn(II) is higher than for Cd(II) and Pb(II), whose sensitivities remain more or less constant and significantly decrease, respectively, compared to pH 6.8. This decrease in the sensitivity in the case of Pb (II)-ion is attributed to the presence of hydrolysis at this pH value. Finally at pH 8.2, the sensitivity for Cd(II) and Pb(II) is comparable to that of pH 7.5, while for Zn(II)-ions the sensitivity slightly decreases probably due to the presence of some hydrolysis. At the view of the results, we can conclude that, regardless of pH value and metal ion, GSH–GEC is the sensor with better sensitivity followed by Cys–Gly–GEC sensor, and being γ-Glu–Cys–GEC the less sensitive sensor. The second observation is that pH can add some discrimination power to resolve the mixture.

3.3. *Quantification of the metal mixtures*

After compression of the data, and in order to find the appropriate ANN model, significant effort is needed to optimize the configuration details that determine its operation. Normally, this is a trial-and-error process, where several parameters (training algorithms, number of hidden layers, transfer functions, etc.) are fine-tuned in order to find the best configuration that optimizes the performance of the model.

Thus, model was built employing the samples from the training subset, and its accuracy was then evaluated towards samples of the external test subset by using the built model to predict the concentrations of the metals of those samples. Since the external test subset data is not employed at all for the modeling, its goodness of fit is a measure of the accomplished modeling performance. To easily check the prediction ability of the obtained ANN model, comparison graphs of predicted vs. expected concentrations for the considered compounds were built, both for training subset and testing subsets. Additionally, root mean square error (RMSE) was also calculated [30]. Thus, the best model will be the one that has the lowest RMSE and regression parameters from the comparison graphs close to the ideal values (i.e. slope and correlation coefficient equal 1, and intercept equal 0).

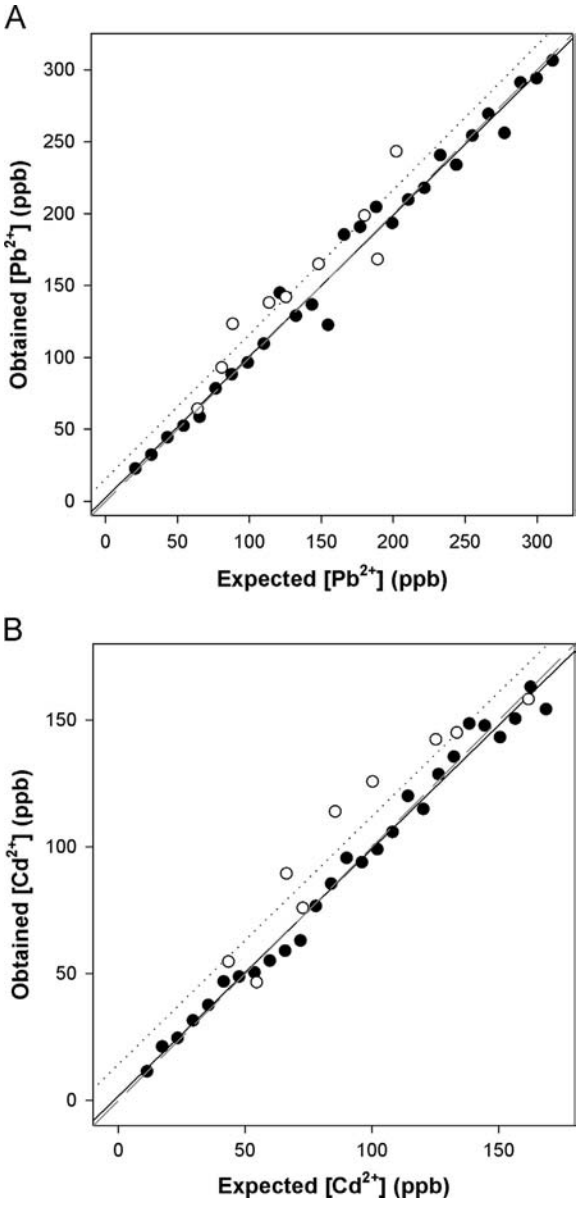

Fig. 4. Modeling ability of the optimized ANN for GSH-GEC sensor at pH 8.2. Sets adjustments of obtained vs. expected concentrations for (A) Pb(II) and (B) Cd(II), both for training (•, solid line) and testing subsets (○, dotted line). Dashed line corresponds to theoretical diagonal line.

3.3.1. One sensor at single pH value

Initially, resolution of the three metals mixtures was attempted employing separately the data from each of the pHs (6.8, 7.5 and 8.2) using the GSH–GEC sensor. The selection of GSH–GEC sensor over the other sensors is motivated by both GSH is constituted by Cys–Gly plus γ-Glu–Cys fragments and presents better performance in voltammetric measurements. In this manner, voltammetric responses obtained on GSH–GEC sensor were compressed employing FFT and three different neural network models were built; i.e. one for each of the pHs. Being the purpose of such approach to assess if data collected from a single pH could be enough to achieve the correct modeling of the three species.

As described, the different ANN models were optimized and comparison graphs were built for each of the cases. However, accuracy of the generated models was too poor (data not shown), especially for zinc, for which either slope or correlation coefficients were around 0.8 in the best cases (expected value of 1.0). These results agreed with the ones that could be expected having a look at the raw voltammetric responses (Fig. 3), as the peak corresponding to zinc is the smallest and distorted one.

Then, based on these results, it was thought that maybe the system would be able to overcome the presence of zinc in the samples and correct its interference for the modeling of the other two metal species; an approach already evaluated in previous cases [31].Thus, new ANN models were built, but in this case, having only two output neurons (one for lead and the other for cadmium concentrations).

In this manner, global performance of the model improved, and satisfactory trend was obtained for the two metals as can be seen in Fig. 4 and Table 3, showing the results obtained with GSH-modified sensor at pH 8.2. Thus, demonstrating the capabilities of the approach and the richness of the data. In this case two metals, Pb(II) and Cd(II) could be predicted, and any distortion produced by the presence of Zn(II) could be corrected. Nevertheless, our goal was to achieve the simultaneous quantification of the three species; hence, the next step was to combine the data obtained from the different pHs and use it to build a unique model.

At this point, prior to proceed to build a model with data coming from different pH values, it would be important to ascertain the reproducibility of the approach. That is, to ensure that measurement of new samples at the same pH would lead to the same results already obtained. To this aim, a new set of samples was prepared and measured again. Then, obtained responses were processed by retraining of the previously built model. That is employing the same procedure for data compression and the optimized ANN topology.

In this way, predicted values in external test subset ($n=9$) from the two independent sets of measurements were compared by means of a Student's paired samples *t*-test. Obtained experimental *t* values were 0.441 and 1.95 for Pb(II) and Cd(II), respectively, while the critical tabulated *t* value with 95% confidence level and 8 degrees of freedom was 2.306. This comparison demonstrates that there are no significant differences between replicated experiments and that the method is reproducible at the 95% level.

3.3.2. One sensor at multi-pH values

A second possibility that arises from the studies done is the use of pH as discriminating variable. Therefore, ANN response models based on the responses from one sensor (GSH-modified) at the three pH tested were evaluated for the resolution of the metal mixture.

Upon completion of an extensive study varying its configurations, the final architecture of the ANN model had 24 neurons (8 Fourier coefficients × 3 pHs) in the input layer, 5 neurons and *purelin* transfer function in the hidden layer and three neurons and *tansig* transfer function in the output layer, providing the concentrations of the three species considered. This configuration was employed with the GSH-GEC sensor, as the one with best overall performance.

As can be observed in Fig. 5, similar behavior as in the previous section is obtained for both lead and cadmium, but significant improvements are achieved for zinc. With this approach, a satisfactory trend is obtained for the three compounds, with regression lines closer to the theoretical ones. Additionally, regression parameters were calculated (Table 3), and as shown by the graphs, a good linear trend is attained for all the cases, but, as expected, with improved behavior for the training subsets due to the fact that this subset has been used to build the model. Despite this, the results obtained for both subsets are close to the ideal values, with intercepts close to 0, and slopes and correlation coefficients close to 1.

Table 3
Results of the fitted regression lines for the comparison between obtained vs. expected values, both for the training and testing subsets of samples and the different metal species (intervals calculated at the 95% confidence level).

	Metal	*Correlation*	*Slope*	*Intercept (ppb)*	*RMSE (ppb)*[c]	*NRMSE (ppb)*[c]	*Total RMSE (ppb)*	*Total NRMSE*
One sensor at single pH values[a]								
tr	Pb(II)	0.992	0.98 ± 0.05	2 ± 10	11.1	0.0390	8.66	0.0369
	Cd(II)	0.994	0.98 ± 0.05	1 ± 5	5.28	0.0348		
ts	Pb(II)	0.940	1.01 ± 0.33	15 ± 46	23.7	0.0973	20.7	0.129
	Cd(II)	0.950	0.98 ± 0.29	14 ± 29	17.2	0.154		
One sensor at multi-pH values[b]								
tr	Pb(II)	0.999	0.95 ± 0.02	8 ± 4	6.03	0.0219	5.44	0.0435
	Cd(II)	0.994	0.94 ± 0.04	5 ± 4	5.73	0.0436		
	Zn(II)	0.990	0.90 ± 0.05	5 ± 3	4.44	0.0575		
ts	Pb(II)	0.977	0.95 ± 0.19	21 ± 26	18.1	0.150	17.7	0.174
	Cd(II)	0.940	0.94 ± 0.31	-11 ± 31	21.3	0.211		
	Zn(II)	0.919	1.06 ± 0.41	4 ± 27	12.4	0.154		
Three-sensor array at multi-pH values								
tr	Pb(II)	0.999	0.95 ± 0.02	8 ± 3	5.72	0.0218	4.72	0.0336
	Cd(II)	0.998	0.92 ± 0.02	7 ± 2	4.85	0.0362		
	Zn(II)	0.996	0.92 ± 0.03	4 ± 2	3.25	0.0400		
ts	Pb(II)	0.978	1.04 ± 0.20	16 ± 28	23.9	0.179	19.2	0.174
	Cd(II)	0.937	0.95 ± 0.32	-11 ± 32	20.5	0.198		
	Zn(II)	0.923	1.00 ± 0.37	6 ± 25	10.9	0.143		

[a] GSH-GEC sensor at pH 8.2.
[b] GSH-GEC sensor.
[c] tr: training subset; ts: testing subset; RMSE: root mean square error; NRMSE: normalized root mean square error.

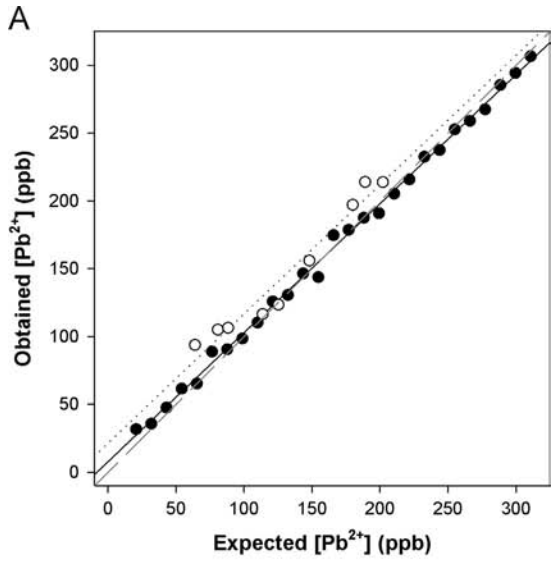

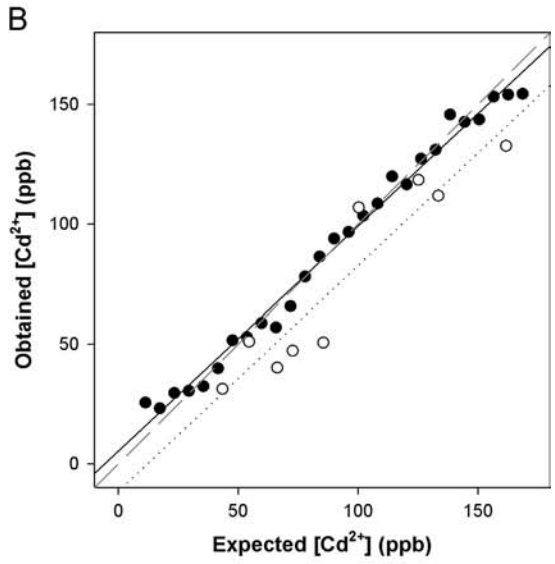

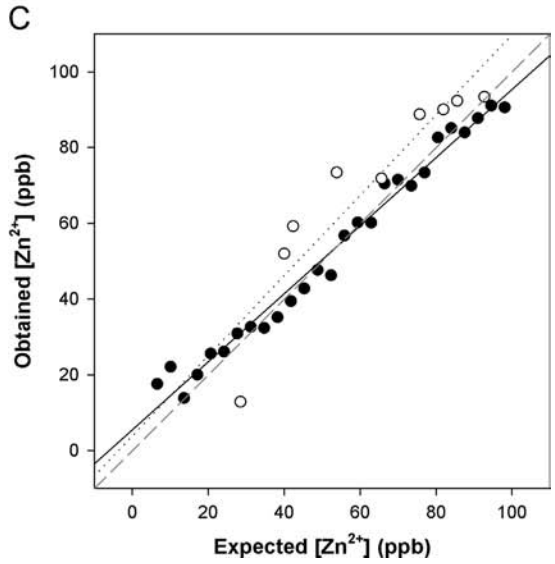

Fig. 5. Modeling ability of the optimized ANN for GSH-GEC sensor using data from the three pHs tested (6.8, 7.5 and 8.2). Sets adjustments of obtained vs. expected concentrations for (A) Pb(II), (B) Cd(II) and (C) Zn(II), both for training (•, solid line) and testing subsets (○, dotted line). Dashed line corresponds to theoretical diagonal line.

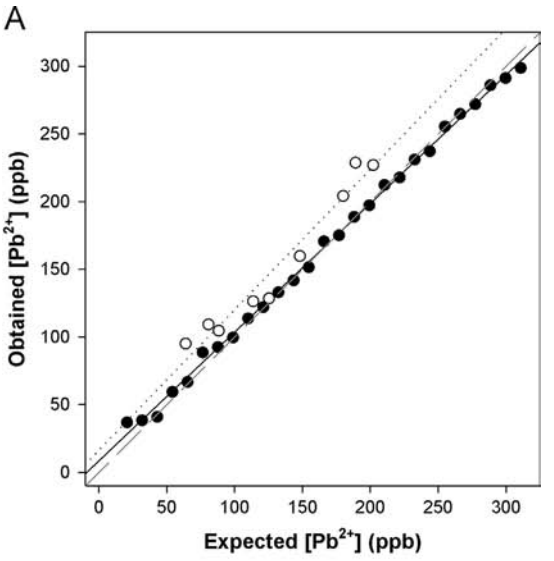

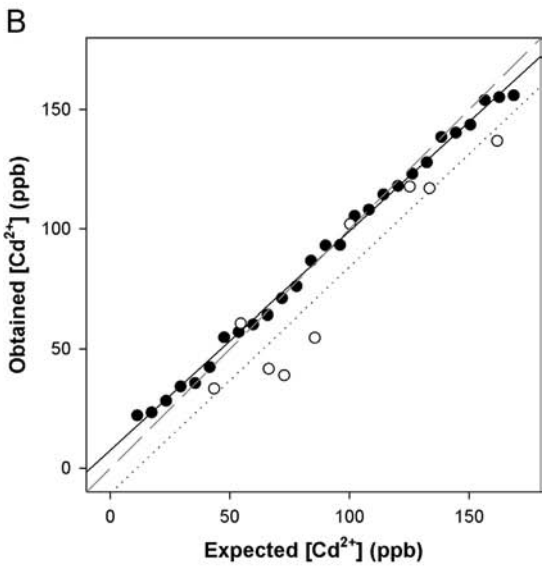

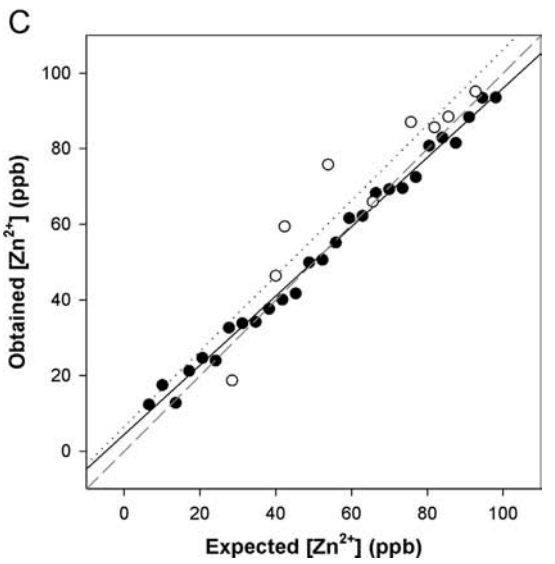

Fig. 6. Modeling ability of the optimized ANN for the three-sensor array at multi-pH values. Sets adjustments of obtained vs. expected concentrations for (A) Pb(II), (B) Cd(II) and (C) Zn(II), both for training (•, solid line) and testing subsets (○, dotted line). Dashed line corresponds to theoretical diagonal line.

3.3.3. Three-sensor array at multi-pH values

Lastly, to further enrich the departure data and try to improve the performance of the generated model, the last approach was based on the use of an array of three electrodes instead of a single sensor. To this aim, the set of samples was measured with the three electrodes (GSH–GEC, γ-Glu–Cys–GEC and Cys–Gly–GEC) and at three different pHs (6.8, 7.5 and 8.2). As the complexity of the data is too high (samples × sensors × pH × potentials), the same approach previously used was employed; that is, unfolding and compression of the recorded voltammograms. In this manner, and after its optimization, the ANN model had 72 neurons (8 Fourier coefficients × 3 pHs × 3 sensors) in the input layer, 4 neurons and *purelin* transfer function in the hidden layer and three neurons and *tansig* transfer function in the output layer, providing the concentrations of the three species considered.

Again, comparison graphs of predicted vs. expected concentrations for the considered compounds were built (Fig. 6) and regression parameters were calculated (Table 3). As it can be seen, results slightly improved in this manner (especially for zinc), but not as much as it could be expected from the increase of the complexity of the voltammetric data. This fact could be mainly due to two reasons; the first one because of GSH is constituted by Cys–Gly and γ-Glu–Cys fragments, and the second one because of the data treatment method. That is, the unfolding of the data may cause discontinuities that, if taken into account, may help on improving the results. However, up to now and to the author's knowledge, there is no method described in the literature for quatrilinear data. Thus, representing this experimental setup a promising field to be explored.

4. Conclusions

At the sight of the results, the simultaneous determination of Pb(II), Cd(II) and Zn(II) at ppb levels was demonstrated using a three-sensor array modified with GSH, γ-Glu–Cys and Cys–Gly. The peptides were successfully immobilized on aryl diazonium salt monolayers anchored on a graphite epoxy composite electrode surface. A good voltammetric response was obtained for all the metals at three experimental pH values using GSH–GEC, γ-Glu–Cys–GEC and Cys–Gly–GEC sensors, although GSH–GEC is the one with better sensitivity followed by Cys–Gly–GEC, and being γ-Glu–Cys–GEC the less sensitive sensor. The concentration intervals of metals, as well as the achieved detection limits are similar to those obtained in previous work [22]. However in this paper the applied deposition time was significantly reduced, being of 300 s instead of the 600 s used in earlier studies. Therefore, lower concentrations ranges and better detection limits could still be achieved by increasing the deposition time. Moreover, attaining better performance of the built models as demonstrated through the reduction of RMSE values.

Comparative analysis of voltammetric data, preprocessed by fast Fourier transform and coupled with an artificial neural network provided by one sensor at both single and multi-pH values with those supplied by the three-sensor array at multi-pH values, allows to conclude that the information provided by GSH–GEC sensor at single pH values was not enough to achieve the correct modeling of the three species. Satisfactory results were only obtained for both Pb(II) and Cd(II) ions, while the presence of zinc in the samples was corrected as an interference by the model. In contrast, the information collected by GSH–GEC sensor at multi-pH values permitted to obtain a satisfactory trend for the three metal ions.

Finally, the analysis of multi-way data from the three-electrode array, which represents a first attempt using quatrilinear data, resulted in a slightly improvement of the results (especially for zinc), but not as much as it could be expected from the increase of the data complexity; this is probably due to redundancy, in the fact that GSH is constituted by Cys–Gly and γ-Glu–Cys fragments, or to the still to improve data treatment. Nevertheless, the followed procedure, as approach to enrich the departure data and to improve the performance of the generated model is a promising field to be explored.

In conclusion, the present work considers a problem that can be encountered in the analysis of natural samples containing a mixture of different heavy metals. Even so, further research focused on the application of the analysis of multi-way data from an array of peptide-modified electrodes for the determination of heavy metals ions in environmental and biological samples is required.

Acknowledgment

The authors acknowledge financial support from the Spanish Ministry of Science and Innovation (MICINN, projects CTQ2010-17099 and CTQ2012-32863) and from the Catalonia program ICREA Academia.

References

[1] J.J. Gooding, D. Hibbert, W. Yang, Sensors 1 (2001) 75–90.
[2] J.J. Gooding, in: S. Alegret, A. Merkoçi (Eds.), Electrochemical Sensor Analysis, Elsevier, Amsterdam, NL, 2007, pp. 189–210.
[3] E. Chow, J.J. Gooding, in: S. Alegret, A. Merkoçi (Eds.), Electrochemical Sensor Analysis, Elsevier, Amsterdam, NL, 2007, pp. e83–e92.
[4] N. Serrano, I. Šestáková, J.M. Díaz-Cruz, C. Ariño, J. Electroanal. Chem. 591 (2006) 105–117.
[5] E. Chekmeneva, R. Prohens, J.M. Díaz-Cruz, C. Ariño, M. Esteban, Anal. Biochem. 375 (2008) 82–89.
[6] R. Gusmão, C. Ariño, J.M. Díaz-Cruz, M. Esteban, Anal. Biochem. 406 (2010) 61–69.
[7] G. Scarano, E. Morelli, Electroanalysis 10 (1998) 39–43.
[8] I. Šestáková, H. Vodičková, P. Mader, Electroanalysis 10 (1998) 764–770.
[9] A. Alberich, C. Ariño, J.M. Díaz-Cruz, M. Esteban, Talanta 71 (2007) 344–352.
[10] E. Chekmeneva, R. Prohens, J.M. Díaz-Cruz, C. Ariño, M. Esteban, Environ. Sci. Technol. 42 (2008) 2860–2866.
[11] R. Gusmão, S. Cavanillas, C. Ariño, J.M. Díaz-Cruz, M Esteban, Anal. Chem. 82 (2010) 9006–9013.
[12] R. Gusmão, C. Ariño, J.M. Díaz-Cruz, M. Esteban, Analyst 135 (2010) 86–95.
[13] S. Cavanillas, R. Gusmão, C. Ariño, J.M. Díaz-Cruz, M. Esteban, Electroanalysis 24 (2012) 309–315.
[14] A. Alberich, N. Serrano, C. Ariño, J.M. Díaz-Cruz, M. Esteban, Talanta 78 (2009) 1017–1022.
[15] V. Sosa, N. Serrano, C. Ariño, J.M. Díaz-Cruz, M. Esteban, Talanta 107 (2013) 356–360.
[16] S.C. McCutcheon, J.L. Schnoor, Phytoremediation: Transformation and Control of Contaminants, John Wiley & Sons Inc, New York, US, 2003.
[17] John Wiley & Sons Inc, New York, US, 1999.
[18] B. Suresh, G.A. Ravishankar, Crit. Rev. Biotechnol. 24 (2004) 97–124.
[19] U.E. Wawrzyniak, P. Ciosek, M. Zaborowski, G. Liu, J.J. Gooding, Electroanalysis 25 (2013) 1461–1471.
[20] M. Delamar, R. Hitmi, J. Pinson, J.M. Saveant, J. Am. Chem. Soc. 114 (1992) 5883–5884.
[21] J.J. Gooding, S. Ciampi, Chem. Soc. Rev. 40 (2011) 2704–2718.
[22] D. Ebrahimi, E. Chow, J.J. Gooding, D.B. Hibbert, Analyst 133 (2008) 1090–1096.
[23] B.H. Cruz-Vásquez, J.M. Díaz-Cruz, C. Arino, M. Esteban, R. Tauler, Analyst 127 (2002) 401–406.
[24] B.H. Cruz Vásquez, J.M. Díaz-Cruz, C. Ariño, M. Esteban, Electroanalysis 15 (2003) 1177–1184.
[25] A.I. Vogel, Textbook of Quantitative Chemical Analysis, 5th ed., Pearson Education Limited, Harlow, GB, 1989.
[26] X. Cetó, J.M. Gutiérrez, L. Moreno-Barón, S. Alegret, M. del Valle, Electroanalysis 23 (2011) 72–78.
[27] C. Ocaña, M. Valle, Microchim. Acta 181 (2014) 355–363.
[28] E. Chow, D.B. Hibbert, J.J. Gooding, Analyst 130 (2005) 831–837.
[29] X. Cetó, F. Céspedes, M.I. Pividori, J.M. Gutiérrez, M. del Valle, Analyst 137 (2012) 349–356.
[30] X. Cetó, F. Céspedes, M. del Valle, Microchim. Acta 180 (2013) 319–330.
[31] A. Mimendia, J.M. Gutiérrez, L.J. Opalski, P. Ciosek, W. Wróblewski, M. del Valle, Talanta 82 (2010) 931–938.